THE JOURNAL OF BIOLOGICAL CHEMISTRY VOL. 286, NO. 15, pp. 13626–13637, April 15, 2011

Combination Treatment with HER-2 and VEGF Peptide Mimics Induces Potent Anti-tumor and Anti-angiogenic Responses *in Vitro* and *in Vivo*[*]

Received for publication, December 27, 2010, and in revised form, February 7, 2011 Published, JBC Papers in Press, February 16, 2011, DOI 10.1074/jbc.M110.216820

Kevin C. Foy[‡§], **Zhenzhen Liu**[¶], **Gary Phillips**[‖], **Megan Miller**[‡§], **and Pravin T. P. Kaumaya**[‡§¶‖1]

From the [‡]*Department of Microbiology,* [¶]*Ohio State Biochemistry Program,* [§]*Department of Obstetrics and Gynecology, and* [‖]*Arthur G. James Comprehensive Cancer Center, Ohio State University, Columbus, Ohio 43210*

HER-2 is a member of the EGF receptor family and is overexpressed in 20–30% of breast cancers. HER-2 overexpression causes increased expression of VEGF at both the RNA and protein levels. HER-2 and VEGF are therefore considered good targets for cancer treatment, which has led to the development of two humanized monoclonal antibodies (mAb) pertuzumab and bevacizumab. Although passive immunotherapy with these Abs are approved for treatment of advanced breast cancer, a number of concerns exist. Treatment is expensive, has a limited duration of action, and is usually accompanied by serious side effects. We hypothesized that therapy with conformational peptide mimics aimed at blocking receptor-ligand interaction is potentially safer with little toxicity, cheaper with a longer half-life, and has greater penetrating abilities than mAbs. We designed and synthesized peptides based on the binding of HER-2 with pertuzumab and VEGF with VEGFR2. We show that treatment with the peptide mimics induces potent anti-tumor responses *in vitro* as determined by cell viability, proliferation, and HER2 phosphorylation assays. We also demonstrate in a transplantable BALB/c mouse tumor model that treatment with the peptide mimics resulted in a greater delay in tumor growth and development. Similarly, treatment with the peptide mimics inhibited angiogenesis *in vivo* as assessed by a Matrigel plug assay. To address the problem of degradability of L-amino acid peptides *in vivo*, we synthesized the retro-inverso D-peptide mimics that resulted in higher efficacy in treatment. Our study shows that combination treatment with HER-2 and VEGF peptide mimics provides greater efficacy than individual treatments.

HER-2 (human epidermal growth factor receptor-2) is a member of the HER family of receptor tyrosine kinases and is overexpressed in about 30% of invasive breast cancers and multiple epithelial tumors (1, 2). HER-2 overexpression is associated with markedly aggressive forms of cancer with a worse prognosis of several malignancies (3, 4) and is therefore considered an important therapeutic target in many cancers for several reasons. The amount of HER-2 expressed on cancer cells is much higher than in normal adult tissues (5), potentially reducing the toxicity of HER-2 targeting drugs. Tumors with a high expression of HER-2 often show homogeneous, intense immunohistochemistry staining (6), signifying that HER-2-targeted therapy would target most cancer cells in a given patient. Additionally, HER-2 overexpression is found in both the primary and metastatic sites (7), suggesting that HER-2 targeted therapy may be effective in all disease sites. HER-2 overexpression and amplification are seen in subsets of gastric, esophageal, endometrial, uterine, ovarian, and lung cancers (8–13). All four HER receptors (EGFR (HER-1), HER-2, HER-3, and HER-4) share structurally homologous extracellular domains (14). HER-2 plays a major coordinating role in this network, because each receptor with a specific ligand seems to prefer HER-2 as its heterodimeric partner (15, 16) due to its constitutively "open" conformation. HER-2-containing heterodimers potently amplify signaling because HER-2 reduces the rate of ligand dissociation, allowing strong activation of downstream signaling pathways (17, 18) and those involving the phosphatidylinositol 3-kinase (PI3K) and MAPK (19). This makes HER-2 a very attractive therapeutic target and also suggests that HER-2-targeted therapy will target most cancer cells in a given patient.

The up-regulation of HER-2 is associated with increased expression of vascular endothelial growth factor or VEGF at both the RNA and protein levels in human breast cancer cells, and exposure of HER-2-positive cells to trastuzumab significantly decreases VEGF expression (20). Shc, a downstream adaptor protein of the HER-2 signaling pathway, has been identified as a critical switch for VEGF production (21) showing that VEGF is a downstream target of the HER-2 signaling pathway. This shows that the effects of HER-2 on tumor cell behavior may be mediated in part through stimulation of angiogenesis. Angiogenesis is the growth of new blood vessels from pre-existing ones and contributes to the development of numerous types of tumors and their metastasis. VEGF, a well known pro-angiogenic factor, is secreted by most tumor cells (22). VEGF expression is increased in many different types of cancer, and most tumor cells secrete VEGF (23). It is also thought that VEGF is a key promoter of metastasis (24). VEGF is a 34–42-kDa, homodimeric, heparin-binding, and disulfide-bonded glycoprotein that has several isoforms arising from splice variants (23, 25–28). VEGF has three known tyrosine kinase receptors as follows: Flt-1 (VEGF-R1), KDR (VEGF-R2, Flk-1), and Flt-4 (VEGF-R3). VEGF-R1 has a higher affinity for VEGF, but it has been shown that VEGF-R2 is the biologically relevant receptor. Therefore, VEGF and its receptors VEGFR-1 and VEGFR-2 are prime targets for anti-angiogenic intervention that is thought

[*] This work was supported, in whole or in part, by National Institutes of Health Grant 84356 from NCI.

[1] To whom correspondence should be addressed: Ohio State University, Ste. 316 Medical Research Facility, 420 W. 12th Ave., Columbus, OH 43210. Tel.: 614-292-7028; Fax: 614-292-1135; E-mail: Kaumaya.1@osu.edu.

to be one of the most promising approaches in cancer therapy. Blocking angiogenesis is an attractive strategy to inhibit tumor growth, invasion, and metastasis. Several monoclonal antibodies have been developed to block VEGF from binding to its receptors, one of which, A4.6.1 or Avastin (bevacizumab), has been approved by the Food and Drug Administration (29). Bevacizumab has been tested in several cancer clinical trials (29–31) and showed some promising results in a phase II clinical trial for breast cancer (20). Other VEGF inhibitors in clinical trials in progress today include several receptor tyrosine kinase inhibitors, VEGF-Trap and anti-VEGF-R2 (21, 29). VEGF stimulates angiogenesis by binding to its receptor VEGFR2 that is expressed by both endothelial and tumor cells (32). A two-pronged approach to target by co-immunizing with defined tumor-associated antigens and angiogenesis-associated antigens has been shown to have synergistic effects (32–34). All of these show that combination treatment targeting both HER-2 and VEGF is a promising strategy because angiogenic therapy alone will only delay tumor growth (35), and targeting HER-2 and VEGF will destroy two different tumor-dependent sub-pathways.

The work described here stems from work conducted in our laboratories over the past decade in developing effective vaccine strategies for HER-2/*neu* (36–41) as well as developing novel therapies based on blockade of receptor-ligand interactions such as B7:CD28 (42–44, 53). Additionally, we have shown that peptide vaccines of the HER-2/*neu* dimerization loop are effective in inhibiting mammary tumor growth *in vivo* (53). We have also developed effective inhibitors of VEGF, VEGFR2 (see accompanying paper (73)). The latter objective was driven by the observation that HER-2 activation induces the expression of VEGF, which is a pro-angiogenic factor making blockade of angiogenesis an attractive and additional strategy to inhibit tumor growth, invasion, and metastasis.

The basic hypothesis in the design of peptide mimics of VEGF and HER-2 is that many proteins exert their biological activity through relatively small regions of their folded surfaces. This approach relies on the premise that the key residues of the binding epitope, in particular side-chain functional groups responsible for a significant portion of the binding affinity to a given receptor/ligand, may be transferred to a much smaller molecule with the contributions to binding largely intact (45). The strategy for the retro-inverso (RI)[2] modification of peptides relies on the synthesis of the sequence using D-amino acids in reverse order (from the N to C termini), such that the resulting peptide mimic has a reversal of the peptide backbone but a topochemical equivalence to the parent peptide in terms of side-chain orientation.

In this study, we report on the studies of the HER-2(266–296) peptide mimic in combination with two VEGF peptide mimics that were synthesized using L- and D-amino acids. The conformational VEGF peptides were shown to mimic the binding site of VEGF to its receptor VEGFR2 (73) by surface plasmon resonance assay. Combination treatments with both peptides were able to cause superior anti-tumor and anti-angiogenic effects *in vitro* and *in vivo*. This dual therapeutic benefit is clearly demonstrated by the increased proliferation and phosphorylation inhibition as well as by a decrease in cell viability. Combination treatment also caused a greater delay in tumor growth and development in a transplantable tumor model. These results indicate that the selected inhibitory peptides have great therapeutic effects in targeting both HER-2 and VEGF by eliciting potent anti-tumor and anti-angiogenic effects.

MATERIALS AND METHODS

Synthesis and Characterization of Conformational Peptides—Peptide synthesis was performed on a Milligen/Biosearch 9600 peptide solid phase synthesizer (Bedford, MA) using Fmoc/*t*-butyl chemistry. Preloaded Fmoc-Val-CLEAR acid resin (0.35 mmol/g) for the 266–296-residue and CLEAR AMIDE resin for the VEGF peptides (0.32 mmol/g) (Peptides International, Louisville, KY) were used for synthesis. The 266–296-residue cyclized epitope was assembled by choosing the regioselective side chain protector Trt on Cys residues 268 and 295 (20), and in the VEGF peptides two cysteines were inserted between amino acid Gln-79 and Gly-92 and between Ile-80 and Glu-93. Peptides were cleaved from the resin using cleavage reagent B (trifluoroacetic acid/phenol/water/TIS, 90:4:4:2), and crude peptides were purified by semi-preparative reversed-phase HPLC and characterized by electrospray ionization mass spectroscopy (46). Intramolecular disulfide bonds were formed using iodine oxidation as described previously (47), and disulfide bridge formation was further confirmed by maleimide-PEO_2-biotin reaction and subsequent analysis using electrospray ionization mass spectroscopy.

Circular dichroism was done as described previously (20). Briefly, aqueous solutions for CD were prepared by dissolving the freeze-dried peptides in appropriate amounts of HPLC water to give a final concentration of 0.5 mM and used as stock solution for further dilution. CD spectra were recorded on an AVIV model 62A DS CD instrument. Mean residue ellipticity ($[\theta]_{M,\lambda}$) values were calculated according to the equation $[\theta]_{M,\lambda} = (\theta \times 100 \times M_r)/(n \times c \times l)$, where θ is the recorded ellipticity (degree); M_r indicates the molecular weight of the peptide; n indicates the number of residues in the peptide; c indicates the peptide concentration (milligrams/ml); and l indicates the path length of the cuvette.

Animals—Female BALB/c mice were purchased from The Jackson Laboratory (Bar Harbor, ME). Animal care and use were in accordance with institutional guidelines.

Cell Lines and Antibodies—All culture media, FBS, and supplements were purchased from Invitrogen. The human breast tumor cell lines BT-474, SK-BR-3, and MDA-468 were purchased from American Type Culture Collection (Manassas, VA) and maintained according to the supplier's guidelines. TUBO cells were a cloned cell line established *in vitro* from a lobular carcinoma that arose spontaneously in a BALB-*neuT* mouse (48). Humanized mouse mAb trastuzumab was generously provided by Genetech, Inc. (South San Francisco, CA).

Statistical Analysis—Tumor growth over time was analyzed using Stata's XTGEE (cross-sectional generalized estimating

[2] The abbreviations used are: RI, retro-inverso; EGFR, EGF receptor; Fmoc, *N*-(9-fluorenyl)methoxycarbonyl; MTT, 3-(4,5-dimethylthiazol-2-yl)-2,5-diphenyltetrazolium bromide; RTK, receptors tyrosine kinase.

equations) model, which fits general linear models that allow you to specify within animal correlation structure in data involving repeated measurements. For other experiments, Student's *t* test was carried out to observe the statistical relevancy between different sets of experiments and the significant difference between treated and nontreated cells.

Proliferation Assay—BT-474, SK-BR-3, MDA-468, and TS/A cells (1×10^4) were plated in 96-well flat-bottom plates overnight. Growth medium was replaced with low sera (1% FCS) medium, and the cells were incubated overnight. Media were removed from the wells and replaced with low sera medium containing HER-2 and VEGF mimic peptides at concentrations ranging from 25 to 150 μg/ml, and plates were incubated an additional 1 h at 37 °C before adding 10 ng/ml HRG in 1% medium. Plates were incubated for an additional 72 h at 37 °C before adding MTT (5 mg/ml) to each well. Plates were incubated for 2 h at 37 °C, and 100 μl of extraction buffer (20% SDS, 50% dimethylformamide (pH 4.7)) was added to each well. Plates were incubated overnight at 37 °C and read on an ELISA reader at 570 with 655 nm background subtraction. Inhibition percentage was calculated as follows: 100% × (untreated cells − peptide-treated cells)/(untreated cells).

Phosphorylation Assay—1×10^6 BT-474 cells were plated in each well of a 6-well plate and incubated overnight at 37 °C. Culture medium was removed and the cell layer washed once with PBS low score (1% FCS). Culture medium was added to the wells, and plates were incubated overnight. Cells were washed, and 50 μg of peptides, anti-peptide Abs, and controls in binding buffer (0.2% w/v BSA, RPMI 1640 medium with 10 mM HEPES (pH 7.2) was added to the wells and incubated at room temperature for 1 h. HRG (5 nM/well) was added, and the incubation was continued for 10 min. Binding buffer was removed, and the cell layer was washed once with PBS before adding 1 ml of RIPA lysis buffer (Santa Cruz Biotechnology, Santa Cruz, CA). Plates were rocked at 4 °C for 2 h. Lysates were removed, spun at 13,000 × *g*, and supernatants collected. Protein concentration of each sample was measured by Coomassie Plus protein assay reagent kit, and lysates were stored at −80 °C. Phosphorylation was determined by Duoset IC for human phosphor-ErbB2 according to the manufacturer's directions (R&D Systems).

Viability Assay—This assay was performed just like the proliferation assay, but after treatment with the peptide inhibitors, the aCella-TOX reagent was used to estimate the amount of dead cells. After peptide treatment for 72 h, the plate was removed and equilibrated to room temperature for 15 min before adding 10 μl of lytic agent to the control wells for maximum lysis and incubated for 15 min at room temperature. 100 μl of the Enzyme Assay Reagent containing Glc-3-P was then added to all wells followed by 50 μl of the detection reagent. The plate was immediately read using a luminometer.

In Vivo Matrigel Assay—500 μl of liquid Matrigel was injected subcutaneously into the flanks of Balb/c mice. The Matrigel (BD Biosciences) contained $VEGF_{165}$ at a final concentration of 500 ng/ml to stimulate angiogenesis and VEGF peptides or irrelevant peptides were added at a concentration of 500 μg/ml. All treatment group contained 3 mice and each mice had two plugs each on the left and right flanks. After 10 days, the mice were sacrificed and Matrigel plugs were removed and hemoglobin content was determined using the Drabkin's reagent kit. The Matrigel plugs were homogenized in hypotonic lysis buffer (250 μl of 0.1% Brij-35 per plug) and centrifuged for 5 min at 5,000 × *g*. The supernatant was incubated at 0.5 ml of Drabkin's solution for 15 min at room temperature, and the absorbance was measured at 540 nm with Drabkin's solution as a blank. Because absorbance is proportional to the total hemoglobin content, the relative hemoglobin content was calculated *versus* the negative and positive controls.

TABLE 1
Amino acid sequences and molecular weight of HER-2 and VEGF peptide mimics

Sequences of amino acids are represented from N to C termini except for the retro inverso peptides RI-HER-2-CYC and VEGF-RI-P4-CYC that were synthesized in the reverse order using D-amino acids. All peptides were synthesized on CLEAR amide resin, using Fmoc/*t*-butyl chemistry. All peptides were acetylated on resin using acetyl-imidazole (4×) in dimethylformamide for 4 h. Cysteine residues are underlined to indicate the locations of the disulfide bonds.

Designation	Peptide	Sequence	M.Wt. (da)
266-HER-2 (CYC)	266-296 L-amino acid cyclized peptide	*CH_3CONH*-(L)-^{266}LHCPA *LVTYNTDTFESMPNPEGRYTFGASCV*^{296}-*CONH2*	2925
RI-HER-2 (CYC)	266-296 D-amino acid cyclized peptide	*CH_3CONH*-D-^{296}VCSAGFTYRGEPNPMSEFTDTNYTVLAPCHL^{266}-*CONH2*	2925
VEGF-P3 (CYC)	76-96 L-amino acid cyclized peptide	*CH_3CONH*-(L)-^{76}ITMQ^{79}-C-^{92}GIHQGQHPKIRMI^{80}-C-^{93}EMSF^{96}-*CONH2*	2527
RI-VEGF-P4 (CYC)	96-76 D-amino acid cyclized peptide	*CH_3CONH*-(D)-^{96}FSME^{93}-C-^{80}IMRIKPHQGQHIG^{92}-C-^{79}QMTI^{76}-*CONH2*	2527

Peptide Treatment in Transplantable Mouse Model—BALB/c mice ($n = 5$) 5–6 weeks of age were challenged subcutaneously with 1×10^5 TUBO cells that express the rat HER-2/*neu*, and after challenge, mice were treated intravenously weekly with 100 μg of either HER-2 or VEGF peptide mimics or a combination of both as inhibitors for a total six treatments. So at day 0, mice are given both the TUBO cells and the first treatment. Mice were euthanized at day 39 post-TUBO challenge (week 10), and tumors were removed. Tumors were measured for tumor volume twice a week using calipers and calculated using the formula (length × width^2)/2. All animal handling was done according to the institutional guidelines.

RESULTS

Selection, Design, Synthesis, and Characterization of Peptides—The selection of the VEGF peptide mimic residues 102–122 (numbered as 76–96 in the crystal structure) corresponds to the overlapping VEGF-binding sites to VEGFR-2 and Avastin. Engineering of this peptide sequence has been described in details elsewhere (73). The sequences of both the HER-2 and VEGF peptide mimics are shown in Table 1. Briefly, the strategy to create a conformational peptide consisting of an anti-parallel β-sheet is described elsewhere (Vicari *et al.* (73)), where the sequence was modified in a way that the resulting peptide VEGF-P3(noncyclized) adopted a conformation very similar to the native structure. It also required two artificial cysteines to

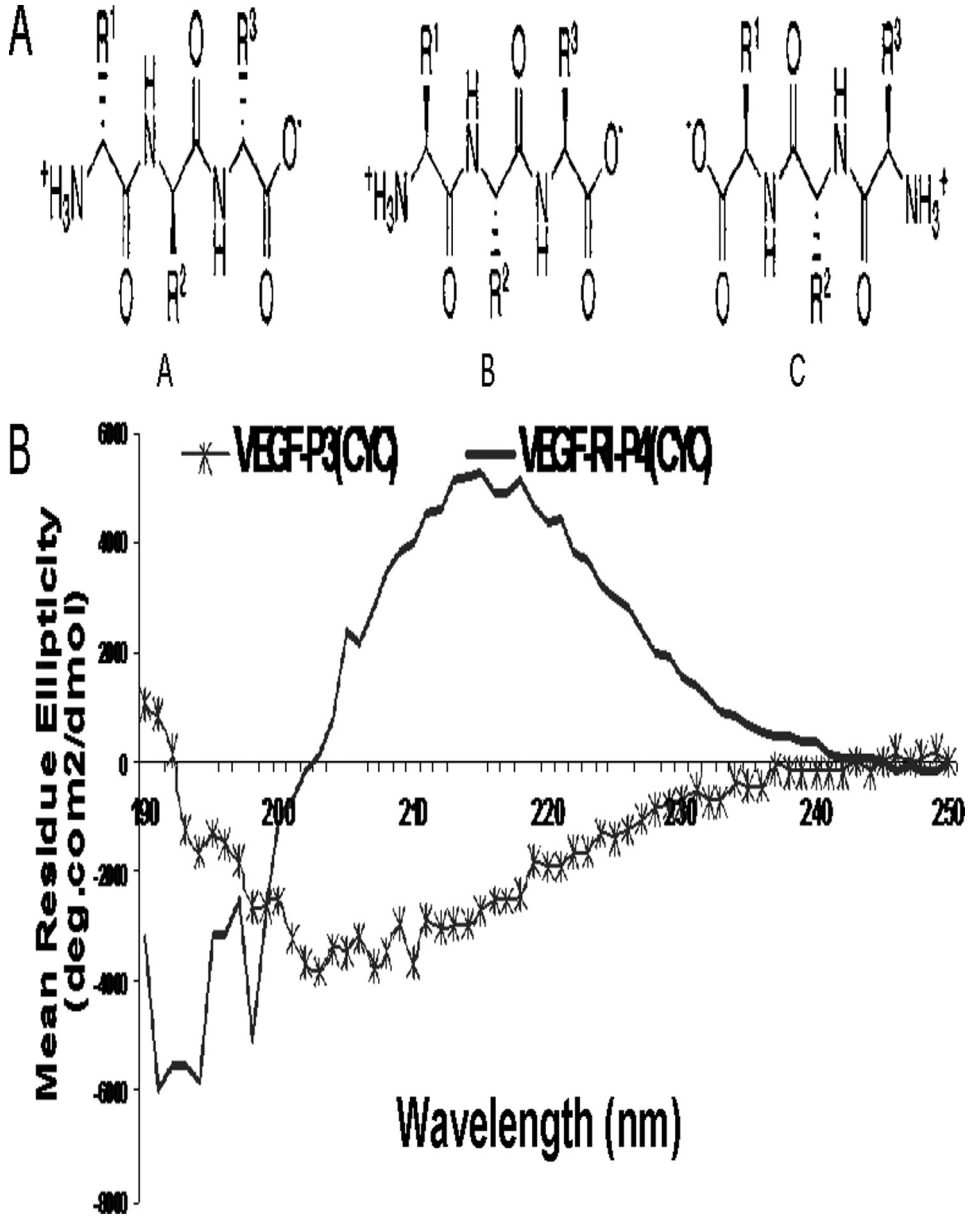

FIGURE 1. *A,* schematic representation of the effects of retro-inverso peptides. Natural orientation of parent L-amino acid peptide (*panel A*). Reversed side chain orientation in D-amino acid peptide (*panel B*). Retro-inverso peptide with restored side chain orientation (*panel C*). *B,* CD spectra of retro-inverso VEGF peptide mimic. CD spectroscopy measurements were made of 100 μM peptide solutions in ether water. Spectra characteristic of β-turn is observed by the shifting of θ mimina toward 217 nm. Inversion of the ellipticity in the spectra was result of inverted chirality by using D-amino acid (RI) resulting in a mirror image profile.

be introduced between Gln-79 and Gly-92 and between Ile-80 and Glu-93. After synthesis and purification of the VEGF-P3(noncyclized) peptide, the disulfide bond was formed by oxidation enabling the formation of the twisted anti-parallel β-sheet structure in the VEGF-P3(CYC). The RI peptide analog VEGF-RI-P4 was synthesized using D-amino acids with the amino acid sequence in reverse order, such that the resulting peptide mimic has a reversal of the peptide backbone but a topochemical equivalence to the parent peptide in terms of side-chain orientation (45, 49, 50). The rationale behind the retro-inverso peptidomimetic is that it should present similar activity with the advantage of higher bioavailability (43). Fig. 1*A* shows a schematic representation of the retro-inverso-D-peptide mimics.

The choice for the HER-2 peptide mimic sequence spanning residues 266–296 (Table 1) was determined first on the basis of the crystal structure of the Fab of pertuzumab bound to the subdomain II of HER-2 extracellular domain (52) and extensive immunogenic studies as described in Ref. 53. The HER-2 peptide mimic 266–296 was selected based on the criteria that antibodies elicited against the peptide were capable of inhibiting dimerization of HER-2 due to its ability to bind and recognize the HER-2 extracellular domain (53). Similar strategies to the VEGF peptide mimic were used to design the HER-2 peptide mimic RI-HER-2 (CYC). All synthetic peptides were successfully synthesized in our laboratory using well established protocols, purified by reversed-phase HPLC using Vydac C-4 column and acetonitrile/water

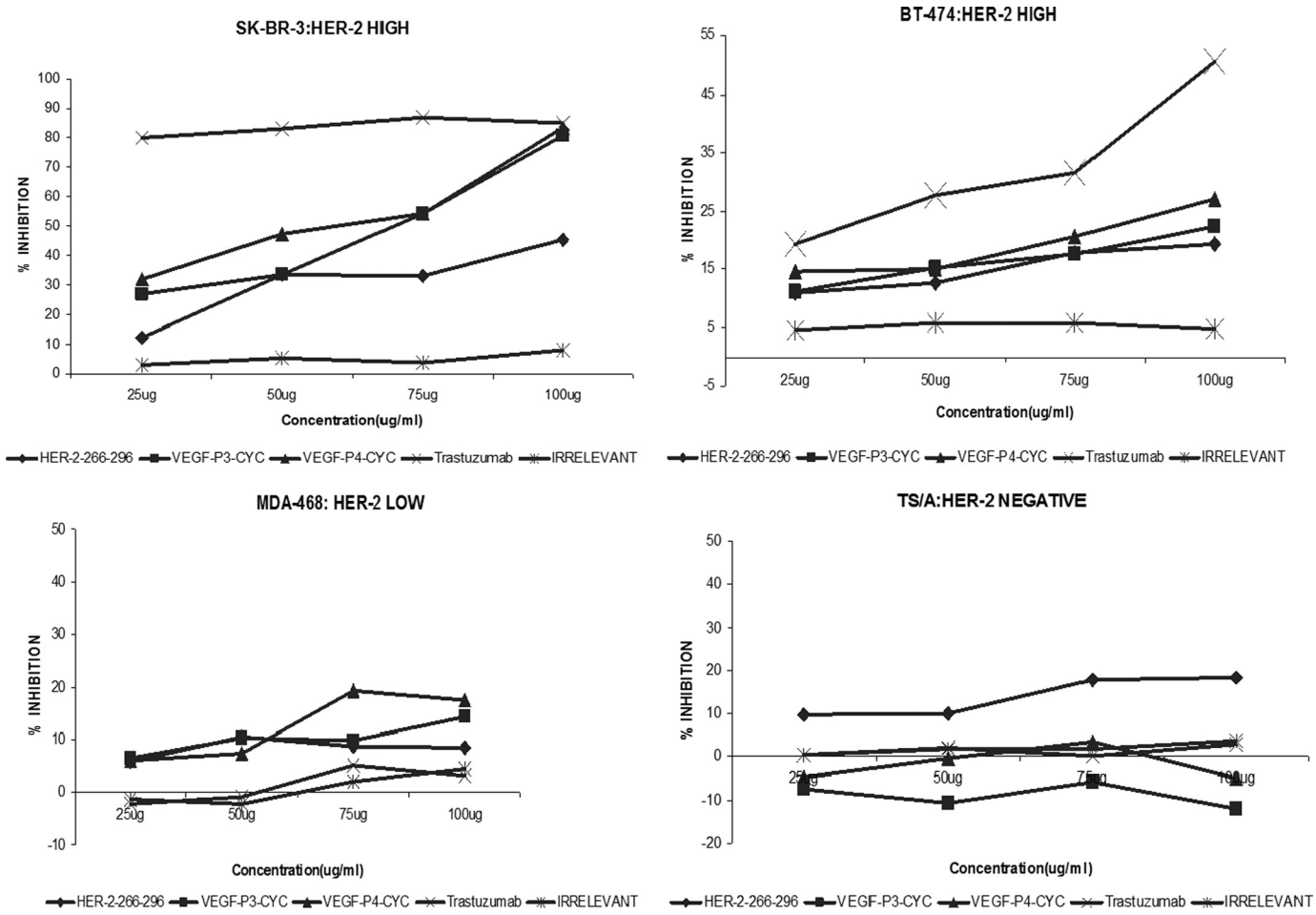

FIGURE 2. **Antiproliferative effects of HER-2 and VEGF peptide mimics used as single treatments.** BT474, SK-BR-3, MDA-468, and TS/A cells were incubated with HER-2 peptide, VEGF peptides, trastuzumab, and irrelevant peptide. Bioconversion of MTT was used to estimate the number of active tumor cells remaining after 3 days. Peptides were added at four different concentrations using the above-mentioned cell lines. The proliferation inhibition rate was calculated using the formula (OD_{normal} untreated − OD peptides or Ab)/OD_{normal} untreated × 100.

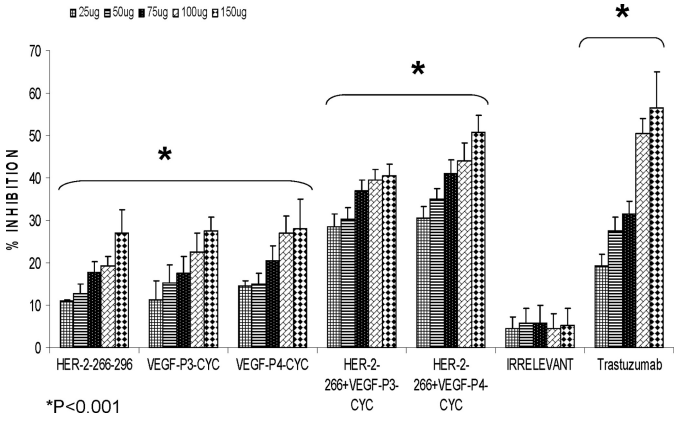

FIGURE 3. **Antiproliferative effects of combination treatment with HER-2 and VEGF peptide mimics.** BT-474 cells were treated in the same manner as in Fig. 2 but treated with HER-2 peptide, VEGF peptides, or a combination of both. Trastuzumab and irrelevant peptide were used as positive and negative controls. Rate of inhibition was calculated using the same formula as above, and all results represent the average of three different experiments. Statistical analysis was done using the analysis of variance model, and * indicates $p <$ 0.001 when compared with the untreated. *Error bars* represent mean ± S.D.

(0.1% TFA) gradient system, and characterized by MALDI spectral analysis. As shown in Fig. 1*B*, the CD spectra is typical of *b*-sheet structure.

Antiproliferative Effects of Peptides—The antiproliferative effects (Fig. 2) of the peptides were tested using four different cell lines (BT-474 and SK-BR-3, HER-2^{high}; MDA-468, HER-2^{low}; and TS/A, HER-$2^{negative}$) in the presence of HRG to activate the HER-3 receptor. Unlike trastuzumab that is specific to HER-2-positive cells, pertuzumab is known to act on cells by disrupting ligand-dependent receptor complexes independent of HER-2/*neu* expression (54). The cells were incubated with the peptides before being exposed to HRG. We found that both the HER-2 and VEGF peptides were able to inhibit tumor growth, and the effect was concentration-dependent (Fig. 2). We used four different cell lines to show that the effects of the peptide were dependent on HER-2 expression because higher inhibition was observed in cases of high HER-2 expression. BT-474 and SK-BR-3 both have high HER-2 expression, but the levels of HER-1 and HER-3 (HER-2 dimerization partners) in SK-BR-3 are, respectively, 10 times and 2 times higher than in BT-474 (55). This probably explains why the % inhibition is by far greater in SK-BR-3 cells than in BT-474 cells (Fig. 2). The HER-2(266–296) also showed inhibitory effects on HER-2 negative cells (TS/A cells), which originated from a mammary adenocarcinoma that arose spontaneously in a BALB/c female retired breeder.

This is because the peptide was designed based on the binding of HER-2 to pertuzumab, which has been shown to inhibit HER-2-negative cells (36).

To determine whether combination treatment would have a significant bearing on inhibition of proliferation as compared with individual treatment, we used mixtures of the HER-2 and VEGF peptide mimics. As shown in Fig. 3, we observed an increase in rate of inhibition when both peptides were used as compared with single treatments (Fig. 3). Statistical analysis showed a significant difference between the treated and untreated cells in all five concentrations (25, 50, 75, 100, and 150 μg) with p values of <0.001 using the 95% confidence intervals. Irrelevant peptide did not show antiproliferative effects, whereas trastuzumab (positive control) showed antiproliferative effects only on cells that express the HER-2 receptor (Figs. 2 and 3).

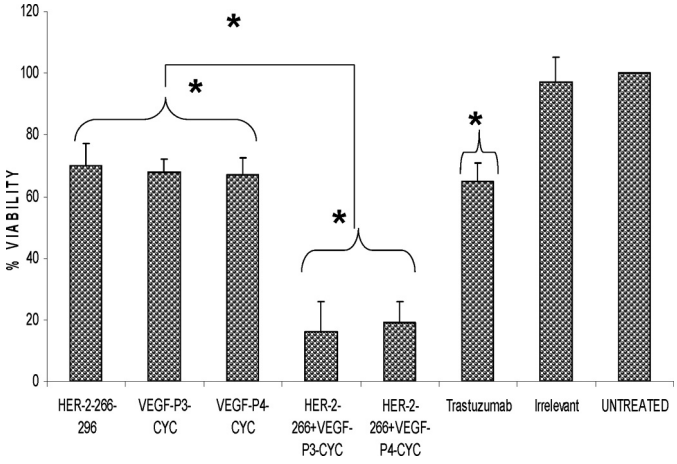

FIGURE 4. **Effects of combination treatment on cancer cell viability.** BT474 cells were incubated with media alone, HER-2 peptide, VEGF peptides, trastuzumab, and irrelevant peptide. The number of viable cells remaining after 3 days was determined using the aCella-TOX reagent kit, and all instructions were done according to the manufacturer's instructions. Cell viability is expressed as a percentage of untreated cells. Data points represent the mean of three independent experiments. *Error bars* represent S.D. Results represent average of three different experiments. Statistical analysis was done using the random effect linear regression model, and * indicates $p < 0.001$ when compared with the untreated and ** indicates $p < 0.001$ when comparing single treatments to combination treatments.

Effects of Peptide Treatment on Breast Cancer Cell Viability—We next evaluated the effects of combination treatment on tumor cell survival *in vitro*. The MTT proliferation assay simply shows that the peptides are able to prevent the cells from growing but does not show whether the cells are being killed by the peptide. This was tested using the acella-TOX reagent kit where dead or dying cells released the enzyme GAPDH, and measuring the activity of this enzyme will give an estimate of the cell viability after treatment. The results showed that the peptide treatment was able to cause a decrease in cell viability, and combination treatment caused a further decrease in viability of at least 40% compared with a single treatment (Fig. 4). There was a statistically significant difference between treatment with HER-2 or VEGF peptides and the untreated group with p values of <0.05 using the 95% confidence interval. The difference was most significant in the case of the combination treatment with both HER-2 and VEGF peptide mimics with p values of <0.001 when using the 95% confidence interval when compared with the untreated. Finally, when comparing the single and combination treatment, we also obtained a significant difference with p values of <0.001 using the same confidence interval. Treatment with irrelevant peptide showed no statistical difference with untreated cells.

Peptide Inhibition of Phosphorylation—The main mode of action of pertuzumab is to inhibit phosphorylation. This is due to the fact that antibody sterically blocks the dimerization

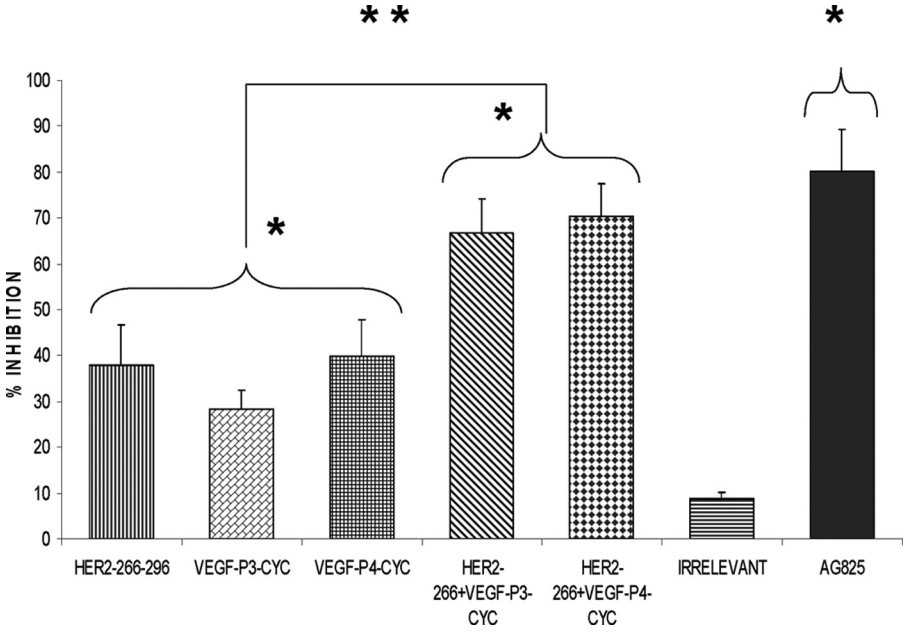

FIGURE 5. **Effects of combination treatment on HER-2 phosphorylation.** BT-474 cells were incubated with 100 μg of HER-2 and VEGF peptides before being exposed to HRG (HER-3-activating ligand) for 10 min and lysed. Phosphorylated HER-2/*neu* was determined by indirect ELISA and percent inhibition was calculated as above. AG825 (Calbiochem), a potent HER-2 phosphorylation inhibitor, was used as a positive control. Results represent average data from three different experiments. *Error bars* represent mean $\pm$ S.D. Statistical analysis was done using the random effect linear regression model, and * indicates $p < 0.001$ when compared with the untreated, and ** indicates $p < 0.001$ when comparing single treatments to combination treatments.

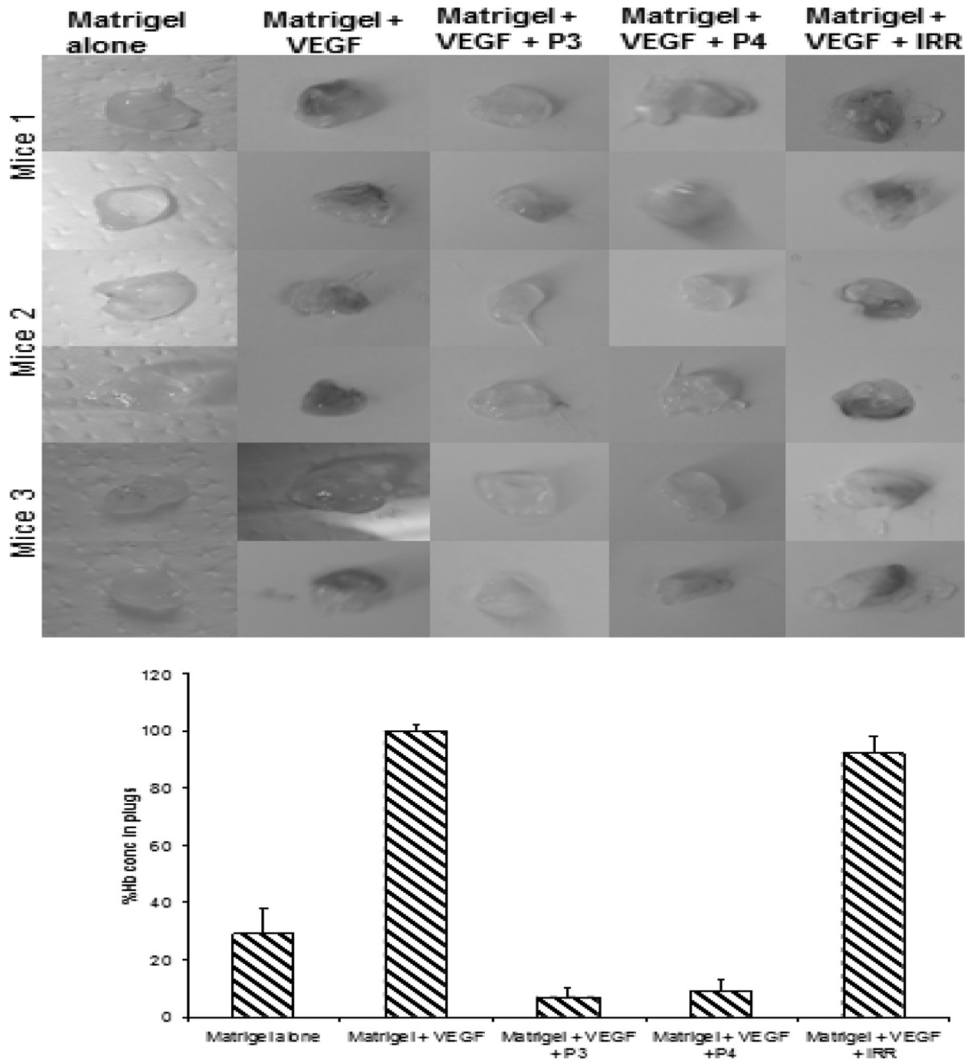

FIGURE 6. **Inhibition of VEGF-dependent angiogenesis in Matrigel plugs by VEGF peptides.** *Top panel, 1st lane,* Matrigel containing PBS alone (−control); *2nd lane,* VEGF (+ control); *3rd lane,* VEGF + P3 peptides; *4th lane,* VEGF + P4, and *5th lane,* VEGF + irrelevant peptide (*VEGF + IRR*) were subcutaneously administered to BALB/c mice on the right and left flanks, and 10 days later the plugs were removed and photos taken as shown. *Bottom panel,* hemoglobin content was determined using Drabskin's method. Each group contained three mice. *Error bars* represent mean ± S.D.

domain of HER-2 thereby preventing the formation of dimers with other HER receptors and thus interrupting downstream signaling. As shown in Fig. 5, the peptides were able to prevent phosphorylation of the HER-2 protein, and single treatment with the HER-2 peptide alone caused a 38% inhibition rate, although the VEGF peptide with L- and D-amino acids caused an inhibition rate of 28 and 39%, respectively. Combination treatments led to dramatic increases in rate of inhibition of 67 and 70% for combining HER-2 + VEGF-P3-CYC and HER-2 + VEGF P4-CYC, respectively (Fig. 5). All peptide treatments were compared with the positive control AG825 (Calbiochem), a HER-2-specific phosphorylation inhibitor. Statistical analysis also showed a significant difference between the treated and untreated groups with p values of <0.001 using the 95% confidence intervals. Also, comparing the single and combination treatments also showed a statistical significant difference between the two treatments with p values of < 0.001. The cells treated with the irrelevant peptide were similar to untreated cells.

In Vivo Matrigel Angiogenesis Assay—To determine whether the VEGF peptides were able to inhibit angiogenesis *in vivo*, we

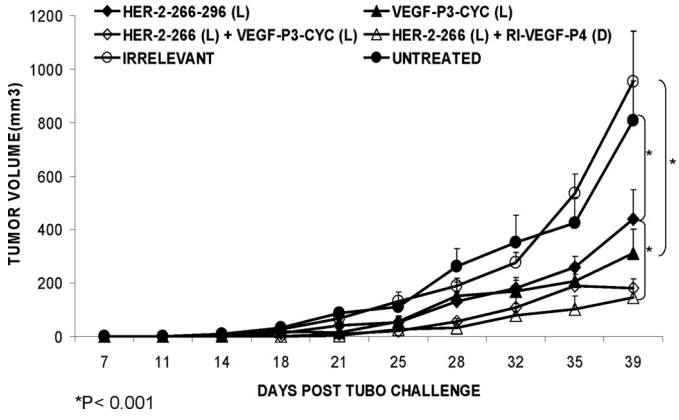

FIGURE 7. ***In vivo* anti-tumor effects of combination treatment with HER-2 L-amino acid peptide.** Wild type BALB/c mice (n = 5), at the age of 5–6 weeks, were challenged with TUBO cells that were derived from BALB-*neuT* mice which are transgenic for the rat HER-2/*neu* oncogene and were treated intravenously with HER-2 and VEGF peptide mimics and scrambled irrelevant peptide. Tumor measurements were performed twice a week using calipers. The data are presented as the average tumor size per group and are reported as 3 mm for combination treatment with HER-2 L-amino acid VEGF peptide mimics.

performed an *in vivo* Matrigel assay in which BALB/c mice were injected with Matrigel containing VEGF and treated with peptide mimics. As shown in Fig. 6, a decrease in hemoglobin content was observed in the case of treatment with VEGF peptide mimics as compared with treatment with an irrelevant peptide or untreated animals. These results indicate that the peptides are able to prevent blood flow to the plugs effectively limiting angiogenesis.

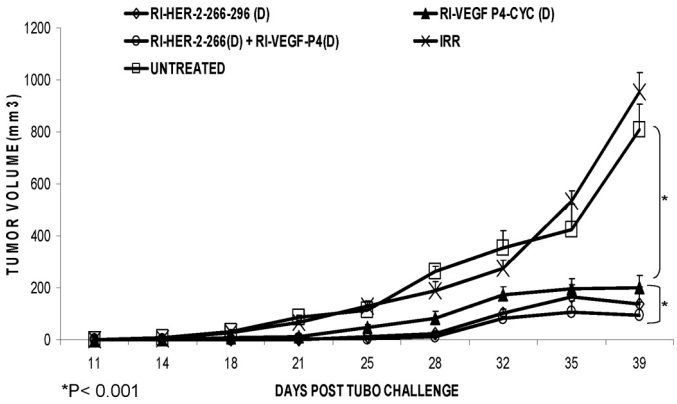

FIGURE 8. ***In vivo* anti-tumor effects of combination treatment with HER-2 D- and VEGF D-amino acid peptide.** Wild type BALB/c mice ($n = 5$) at the age of 5–6 weeks were challenged with TUBO cells that were derived from BALB-*neuT* mice that are transgenic for the rat HER-2/*neu* oncogene and were treated intravenously with HER-2 and VEGF peptide mimics and scrambled irrelevant peptide. Tumor measurements were performed twice a week using calipers. The data are presented as the average tumor size per group and are reported as 3 mm for combination treatment with HER-2 D-amino acid VEGF peptide mimics.

Transplantable Tumor Challenge Models—To determine the ability of the peptides to inhibit tumor growth *in vivo*, we used a rat *neu*-expressing tumor challenge model. The rat *neu* has a 97% similarity to that of the human HER-2(266–296) sequence with only one disparate amino acid (20). To investigate the efficacy of peptide treatment, we challenged groups of BALB/c mice ($n = 5$) with TUBO cells derived from tumors of BALB-*neuT* transgenic mice (23) followed by weekly treatment with either HER-2 or VEGF peptide mimics or a combination of both and monitored tumor growth up to 5–6 weeks post-challenge.

As shown in Fig. 7, combination treatment with HER-2(266–296) (L) peptide mimic with VEGF peptide mimics (VEGF-P3-CYC-(L) or VEGF-P4-(D) produces greater anti-tumor effects as compared with single HER-2 or VEGF peptide mimic treatment. Mice that were treated with the HER-2 peptide alone were significantly different from the group treated with combi-

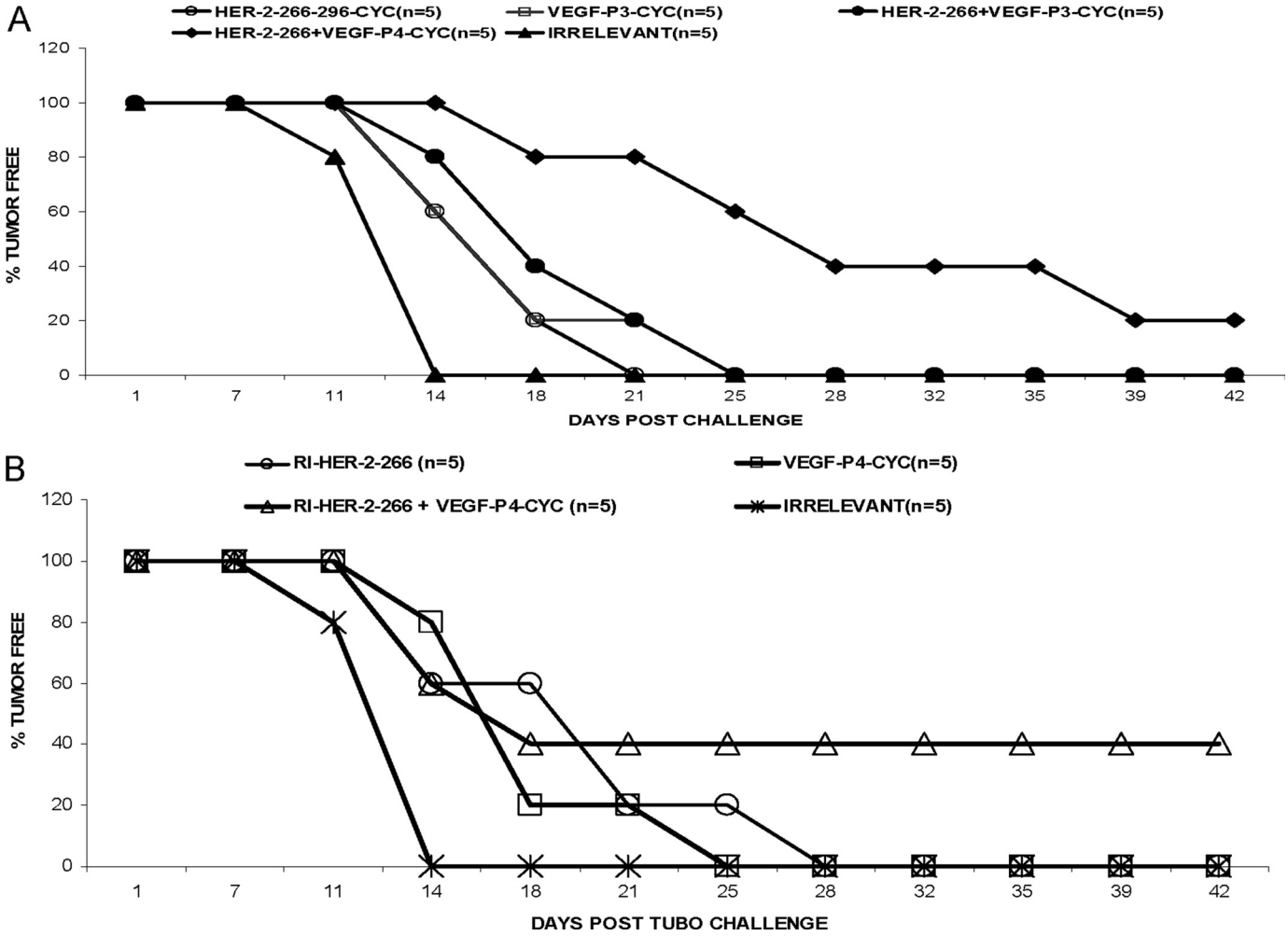

FIGURE 9. **Tumor-free survival rates for combination treatments with HER-2 and VEGF peptide mimics.** Mice were monitored for tumor development twice weekly in both cases of combination treatment with L-amino HER-2 peptide (*A*) and D-amino HER-2 peptide (*B*). In both cases, combination treatment showed the best tumor-free survival rates as compared with single treatments and untreated.

nation of HER-2 and VEGF peptide mimics ($p < 0.001$). There was also a significant delay in onset of tumor development in the case of combination treatment (around day 25) as compared with single treatment (around day 18).

Next, we compared *in vivo* anti-tumor effects with all D-retro-inverso peptide mimics. As shown in Fig. 8, combination treatment with HER-2 D-amino retro inverso peptide and the VEGF-RI-P4 peptide shows greater inhibitory effects than treatment with HER-2 peptide alone. Mice treated with the combination were significantly different from those treated with either the HER-2 peptide alone or the VEGF peptide alone ($p < 0.001$). There was also a delay in onset of tumor development in the case of combination treatment (around day 28) as compared with single treatment (around day 21). These groups also produced a delay in tumor burden, and the group treated with HER-2 and D-amino acid VEGF peptide was 20% tumor-free at the end of the experiment (Fig. 9*A*). The same combination treatment group using the D-amino acid VEGF peptide and HER-2 peptide produced the most statistical significant reduction in the percent tumor weight ($p < 0.001$) using analysis of variance (Fig. 9*B*). There was no significant difference or delay in tumor growth between the untreated and the irrelevant peptide, and tumor growth and development followed a similar pattern.

These results strongly indicate that combination treatment with HER-2 and VEGF peptide mimics produced statistically significant reduction in tumor growth and development *in vivo* and also showed more potent anti-tumor effects in *in vitro* assays indicating that targeting both HER-2 and VEGF is a more attractive strategy than targeting only one of the pathways. Also, the retro inverso D-amino acid peptide mimics gave better results than the L-amino acid peptides in both the cases of single and combination treatments. Additionally, as shown in Fig. 9, combination treatment causes a decrease in tumor burden as illustrated by the % tumor weight in the mice treated with both peptides. The best results were obtained in the case of combination of both the D-amino acids peptides of HER-2 and VEGF with a significant value of $p < 0.001$ as compared with their individual treatments with $p < 0.0047$ when compared with the untreated.

DISCUSSION

Research in our laboratory over the past 2 decades has focused mostly on the development of B-cell epitope vaccines that activate both the humoral and cellular arms of the immune system resulting in the production of high affinity anti-peptide antibodies with enhanced anti-tumor activities. HER-2/*neu* is an oncoprotein that is overexpressed in many types of tumors and is associated with highly aggressive forms of cancers (56, 57). HER-2 is thus an important therapeutic target, and therapeutic modalities have been devised that target the receptor and downstream molecular pathways. We have successfully translated our extensive HER-2 preclinical studies (36, 37) to the clinic in a phase 1 trial (58). Structural studies of HER-2 in complex with the anti-HER-2 antibodies trastuzumab/Herceptin® and pertuzumab/Omnitarg™ have significantly provided new insights into how these drugs function (52). We have designed several conformational peptides based on the binding of the extracellular domain of HER-2 with pertuzumab (53) and trastuzumab (59) as vaccine candidates, which is the subject of an upcoming clinical trial at The James Cancer Hospital (Columbus, OH).

Many therapeutic modalities targeting receptors tyrosine kinases (RTK) and downstream molecular pathways have been devised, and most outstanding among these are the ErbB and vascular endothelial growth factor receptor (VEGFR) families of kinases (26, 30, 60). Many agents have been developed aimed at targeting RTKs, and these include therapeutic antibodies to RTK ligands or the receptors themselves and small molecule inhibitors that target the intracellular kinase domains of RTKs (61–63). Many of the Food and Drug Administration-approved therapies targeting both HER-2 (trastuzumab, Herceptin®) and VEGF (bevacizumab, Avastin) have significant toxicities, including cardiac dysfunction and congestive heart failure (64–66), and many of the patients demonstrate disease progression because of development of resistance. Clinical applications of mAb therapy in general is limited by a number of concerns such as frequency of treatments, associated costs, limited duration of action, undesired immunogenicities, development of resistance, and significant risk of cardiotoxicities (67). Similarly, the small molecule RTK inhibitors such as sunitinib, which have entered clinical trials alone or in combination with radiotherapy or chemotherapy, show problems of efficacy, development of resistance, and unacceptable safety profiles that continue to hamper their clinical progress (65). Despite the success of these drugs, there still remains a high and unmet need for novel molecular cancer therapeutics. Novel therapies targeting these aberrant molecular pathways are urgently needed that can offer hope that the effectiveness and duration of response can be greatly improved.

In this study, we were interested in extending our approaches by evaluating therapy with peptide mimics designed to inhibit the interaction between receptor and its ligand as immunotherapeutic strategies. Given the present state of small molecule inhibitors and their unacceptable safety profiles, we believe that rational synthetic peptide approach may offer a viable and safe alternative. Peptide mimics offer the benefits of being water-soluble, nonimmunogenic, and the ability to easily cross tissue barriers (68). One of the major drawbacks of using peptides as therapy is their high susceptibility to proteosomal degradation (69). Because retro-inverso peptides are synthesized with D-amino acids and proteases usually recognize L-amino acids, they should be resistant to proteosomal degradation and therefore will increase the bioavailability of the peptidomimetic therapeutic *in vivo* (44, 69, 70). As demonstrated in our companion paper (73), our interest in VEGF stems from the fact that overexpression of HER-2 is associated with increased expression of VEGF at both the RNA and protein levels in breast cancer cells, and a positive association between HER-2 and VEGF expression in breast cancer patients has been identified (71). Targeting these two receptors using a combination strategy can result in a synergistic/additive manner killing tumor cells and retarding tumor development (32–34). Thus, combination therapy targeting both HER-2 and VEGF is a very promising strategy because anti-angiogenic therapy alone will only delay tumor growth (35) and targeting HER-2 and VEGF will destroy two

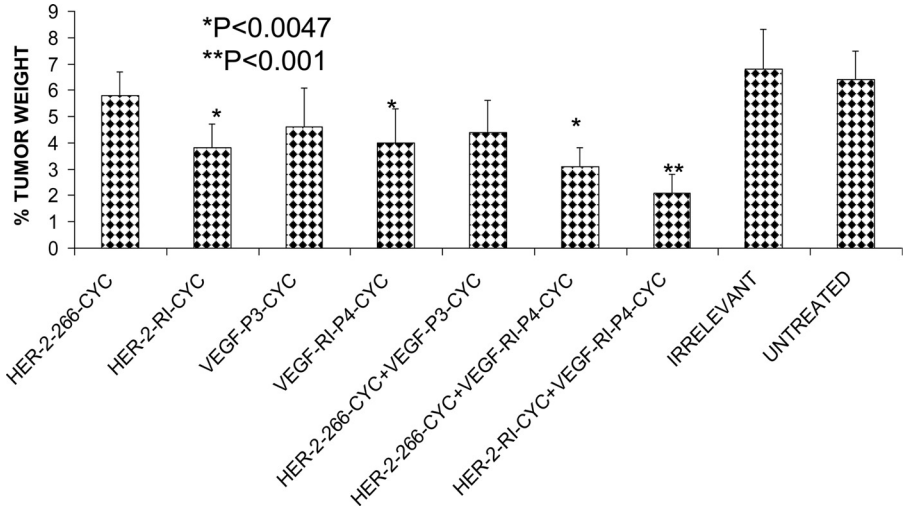

FIGURE 10. **Effects of combination treatment on tumor weight.** Wild type BALB/c mice ($n = 5$), after TUBO challenge and treatment, were sacrificed at day 39, and the weight of the mice with the tumors was measured and recorded. The tumors were then extracted and also measured, and the data were used to calculate the % tumor weight. Results showed a greater reduction in % tumor weight in the cases of combination treatment with the best results observed in the case of combination with both retro inverso D-amino acid peptides. *Error bars* represent mean ± S.D.

different tumor-dependent pathways. As shown in our companion paper (73), we have successfully designed peptide mimics of VEGF to inhibit angiogenesis. This peptide was synthesized and tested in a number of different studies using cancer cells, human umbilical vein endothelial cells, and animal models (73), resulting in the choice of VEGF-P3-CYC.

The retro-inverso analog of the VEGF peptide was designed and synthesized using D-amino acids with the intent that it would be superior to the L-amino acid peptide mimic when used *in vivo*. Pertuzumab binds to different epitopes in the HER-2 extracellular domain, amino acids 266–333, near the junction of domains I–III (52). This interaction was shown to sterically hinder the association of HER-2 with other receptors such as HER-3 sterically blocking a pocket necessary for receptor dimerization and signaling. Based on these studies, we have selected one HER-2 peptide mimic pertuzumab-like sequence 266–296, which has been shown to be a good candidate for a neutralizing peptide (53).

We evaluated the antiproliferative effects of the peptides or their combinations on different cell lines. Trastuzumab has been shown to be specific to only HER-2-positive cells, and this was observed in our results where no inhibition was observed with the TS/A(HER-2-negative) cell line. There was also a reduction in % inhibition in the case of MDA-468 (HER-2 low) as compared with BT-474 and SK-BR-3 (HER-2 high) cells. This indicates that the peptides were effective in inhibiting HER-2 cancer cells. The HER(2–266) peptide showed inhibitory effects also on the HER-2-negative cell line (TS/A), and this is because it is the pertuzumab-like peptide, and pertuzumab is also effective in cells that are independent of HER-2. After showing some level of specificity to the HER-2 receptor, we tested the effects of combination treatment with both HER-2 and VEGF peptides. We noticed that there was an increase in proliferation and inhibition when combination treatment was used, and the treated groups were statistically different from the untreated, but the irrelevant peptide had no statistical effects on the cells (Figs. 2 and 3).

We also evaluated the effects of combination treatment on cell viability, and the results obtained showed that single treatment with HER-2 or VEGF peptides gives a viability of about 70%, whereas combination treatment with both peptides reduces the viability to less than 25% (Fig. 4). The difference was statistically significant between the single and combination treatment with p values of <0.001. HER-2 is known to dimerize with its partners HER-1 and HER-3 leading to receptor phosphorylation and intracellular signaling, and pertuzumab mainly functions by sterically blocking this receptor from binding to its partners and is therefore classified as a dimerization inhibitor (51, 72). We therefore wanted to investigate the effects of peptide treatment on phosphorylation, and the results also indicated an increase in phosphorylation inhibition from less than 40% in the case of single treatments to about 70% in the case of combination treatment, and the differences between these two treatments were statistically significant with p values of <0.001 (Fig. 5).

Efficient *in vivo* angiogenesis assays to assess and compare anti-angiogenic activity are a prerequisite for the discovery and characterization of anti-angiogenic targets. When VEGF are mixed with Matrigel and injected subcutaneously into mice, endothelial cells migrate into the gel plug. These endothelial cells form vessel-like structures, a process that mimics the formation of capillary networks. To delineate whether our results in BALB/c mice were due to inhibition of angiogenesis, we carried out experiments in which we injected Matrigel, Matrigel containing VEGF, and used P3, P4, and an irrelevant peptide as inhibitors (see Fig. 6). The results are clear that there was significant inhibition of hemoglobin content in the plugs treated with the VEGF peptides. This indicates that angiogenesis was significantly inhibited and points to the importance of targeting VEGF and tumor angiogenesis for the treatment of human cancer.

To evaluate the effects of peptide treatment *in vivo*, we used a transplantable mouse model. BALB/c mice were challenged with TUBO cells and treated with peptides and their combina-

tions. The results obtained indicated a statistical significance of $p < 0.001$ between the group treated with the peptides and their combinations and the group treated with the irrelevant peptide or untreated (Fig. 7). Combination treatment with HER-2 D-amino acid RI peptide and the VEGF-P4 peptide showed greater inhibitory effects than treatment with HER-2 peptide alone (Fig. 9). Combination treatment increases the tumor-free survival rates and onset of tumor emergence because 20% of mice in the group treated with HER-2 L-amino acid and VEGF-P4 remained tumor-free at the end of the experiment (Fig. 9*A*), whereas 40% of mice in the group treated with HER-2 D-amino acid and the VEGF-P4 also remained tumor-free at the end of the experiment (Fig. 9*B*). Combination treatment causes a decrease in tumor burden as illustrated by the % tumor weight in the mice treated with both peptides. The best results were obtained in the case of combination of both the D-amino acid peptides of HER-2 and VEGF with a significant value of $p < 0.001$ as compared with their individual treatments with $p < 0.0047$ when compared with the untreated (Fig. 10).

In summary, these data greatly illustrate that the peptide mimics have potent anti-tumor activity, and combination treatment with both HER-2 and VEGF peptides mimics produces additive effects. This shows that targeting the two different receptors will produce greater anti-tumor and anti-angiogenic effects both *in vitro* and *in vivo*. Furthermore, our *in vivo* results point to the treatment efficacy of HER-2 and VEGF combination of the D-amino peptide mimics. These results support our hypothesis that the D-amino peptide exhibits greater *in vivo* stability because it cannot be degraded by proteases. In conclusion, our results may have significant implications and provide viable safe alternatives to present treatment and hold tremendous potential for the treatment of various solid tumor types. Tailored treatments consisting of combinations of vaccines, targeted therapies, angiogenesis inhibitors, and metronomic chemotherapy will hopefully result in better patient outcomes with little toxicity events. Integration of novel agents targeting VEGF, HER-2, and EGFR with the goal to predict which specific targeted agent combinations will most likely benefit individual patients remains a formidable challenge but certainly an attainable goal in the future.

REFERENCES

1. Slamon, D. J., Clark, G. M., Wong, S. G., Levin, W. J., Ullrich, A., and McGuire, W. L. (1987) *Science* **235,** 177–182
2. Slamon, D. J. (1987) *N. Engl. J. Med.* **317,** 955–957
3. Hynes, N. E., and Stern, D. F. (1994) *Biochim. Biophys. Acta* **1198,** 165–184
4. Scholl, S., Beuzeboc, P., and Pouillart, P. (2001) *Ann. Oncol.* **12,** S81–S87
5. Press, M. F., Cordon-Cardo, C., and Slamon, D. J. (1990) *Oncogene* **5,** 953–962
6. Paik, S., Hazan, R., Fisher, E. R., Sass, R. E., Fisher, B., Redmond, C., Schlessinger, J., Lippman, M. E., and King, C. R. (1990) *J. Clin. Oncol.* **8,** 103–112
7. Niehans, G. A., Singleton, T. P., Dykoski, D., and Kiang, D. T. (1993) *J. Natl. Cancer Inst.* **85,** 1230–1235
8. Mimura, K., Kono, K., Hanawa, M., Mitsui, F., Sugai, H., Miyagawa, N., Ooi, A., and Fujii, H. (2005) *Br. J. Cancer* **92,** 1253–1260
9. Morrison, C., Zanagnolo, V., Ramirez, N., Cohn, D. E., Kelbick, N., Copeland, L., Maxwell, G. L., Maxwell, L. G., and Fowler, J. M. (2006) *J. Clin. Oncol.* **24,** 2376–2385
10. Yano, T., Doi, T., Ohtsu, A., Boku, N., Hashizume, K., Nakanishi, M., and Ochiai, A. (2006) *Oncol. Rep.* **15,** 65–71
11. Cirisano, F. D., and Karlan, B. Y. (1996) *J. Soc. Gynecol. Investig.* **3,** 99–105
12. Berchuck, A., Rodriguez, G., Kinney, R. B., Soper, J. T., Dodge, R. K., Clarke-Pearson, D. L., and Bast, R. C., Jr. (1991) *Am. J. Obstet. Gynecol.* **164,** 15–21
13. Kern, J. A., Schwartz, D. A., Nordberg, J. E., Weiner, D. B., Greene, M. I., Torney, L., and Robinson, R. A. (1990) Cancer Res. **50,** 5184–5187
14. Barbacci, E. G., Guarino, B. C., Stroh, J. G., Singleton, D. H., Rosnack, K. J., Moyer, J. D., and Andrews, G. C. (1995) *J. Biol. Chem.* **270,** 9585–9589
15. Tzahar, E., Waterman, H., Chen, X., Levkowitz, G., Karunagaran, D., Lavi, S., Ratzkin, B. J., and Yarden, Y. (1996) *Mol. Cell. Biol.* **16,** 5276–5287
16. Graus-Porta, D., Beerli, R. R., Daly, J. M., and Hynes, N. E. (1997) *EMBO J.* **16,** 1647–1655
17. Beerli, R. R., Graus-Porta, D., Woods-Cook, K., Chen, X., Yarden, Y., and Hynes, N. E. (1995) *Mol. Cell. Biol.* **15,** 6496–6505
18. Graus-Porta, D., Beerli, R. R., and Hynes, N. E. (1995) *Mol. Cell. Biol.* **15,** 1182–1191
19. Olayioye, M. A., Neve, R. M., Lane, H. A., and Hynes, N. E. (2000) *EMBO J.* **19,** 3159–3167
20. Rugo, H. S. (2004) *Oncologist* **9,** Suppl. 1, 43–49
21. Holash, J., Davis, S., Papadopoulos, N., Croll, S. D., Ho, L., Russell, M., Boland, P., Leidich, R., Hylton, D., Burova, E., Ioffe, E., Huang, T., Radziejewski, C., Bailey, K., Fandl, J. P., Daly, T., Wiegand, S. J., Yancopoulos, G. D., and Rudge, J. S. (2002) *Proc. Natl. Acad. Sci. U.S.A.* **99,** 11393–11398
22. Riemer, A. B., Klinger, M., Wagner, S., Bernhaus, A., Mazzucchelli, L., Pehamberger, H., Scheiner, O., Zielinski, C. C., and Jensen-Jarolim, E. (2004) *J. Immunol.* **173,** 394–401
23. Ferrara, N. (2004) *Oncologist* **9,** Suppl. 1, 2–10
24. Saito, H., Tsujitani, S., Ikeguchi, M., Maeta, M., and Kaibara, N. (1998) *Br. J. Cancer* **78,** 1573–1577
25. Hoeben, A., Landuyt, B., Highley, M. S., Wildiers, H., Van Oosterom, A. T., and De Bruijn, E. A. (2004) *Pharmacol. Rev.* **56,** 549–580
26. Houck, K. A., Ferrara, N., Winer, J., Cachianes, G., Li, B., and Leung, D. W. (1991) *Mol. Endocrinol.* **5,** 1806–1814
27. Tischer, E., Mitchell, R., Hartman, T., Silva, M., Gospodarowicz, D., Fiddes, J. C., and Abraham, J. A. (1991) *J. Biol. Chem.* **266,** 11947–11954
28. Ferrara, N., and Henzel, W. J. (1989) *Biochem. Biophys. Res. Commun.* **161,** 851–858
29. Ferrara, N., Hillan, K. J., Gerber, H. P., and Novotny, W. (2004) *Nat. Rev. Drug Discov.* **3,** 391–400
30. Cobleigh, M. A., Langmuir, V. K., Sledge, G. W., Miller, K. D., Haney, L., Novotny, W. F., Reimann, J. D., and Vassel, A. (2003) *Semin. Oncol.* **30,** 117–124
31. Yang, J. C., Haworth, L., Sherry, R. M., Hwu, P., Schwartzentruber, D. J., Topalian, S. L., Steinberg, S. M., Chen, H. X., and Rosenberg, S. A. (2003) *N. Engl. J. Med.* **349,** 427–434
32. Casella, I., Feccia, T., Chelucci, C., Samoggia, P., Castelli, G., Guerriero, R., Parolini, I., Petrucci, E., Pelosi, E., Morsilli, O., Gabbianelli, M., Testa, U., and Peschle, C. (2003) *Blood* **101,** 1316–1323
33. Carpenito, C., Davis, P. D., Dougherty, S. T., and Dougherty, G. J. (2002) *Int. J. Radiat. Oncol. Biol. Phys.* **54,** 1473–1478
34. Monsky, W. L., Mouta Carreira, C., Tsuzuki, Y., Gohongi, T., Fukumura, D., and Jain, R. K. (2002) *Clin. Cancer Res.* **8,** 1008–1013
35. Kim, D. W., Huamani, J., Fu, A., and Hallahan, D. E. (2006) *Int. J. Radiat. Oncol. Biol. Phys.* **64,** 38–46
36. Dakappagari, N. K., Douglas, D. B., Triozzi, P. L., Stevens, V. C., and Kaumaya, P. T. (2000) *Cancer Res.* **60,** 3782–3789
37. Dakappagari, N. K., Pyles, J., Parihar, R., Carson, W. E., Young, D. C., and Kaumaya, P. T. (2003) *J. Immunol.* **170,** 4242–4253
38. Dakappagari, N. K., Sundaram, R., Rawale, S., Liner, A., Galloway, D. R., and Kaumaya, P. T. (2005) *J. Pept. Res.* **65,** 189–199
39. Dakappagari, N. K., Lute, K. D., Rawale, S., Steele, J. T., Allen, S. D., Phillips, G., Reilly, R. T., and Kaumaya, P. T. (2005) *J. Biol. Chem.* **280,** 54–63
40. Steele, J. T., Allen, S. D., and Kaumaya, P T. (2006) in *Cancer Immunotherapy with Rationally Designed Synthetic Peptides* (Kastin, A., ed) Academic Press, Burlington, MA

41. Kaumaya, P. T. (2006) *Int. J. Pept. Res. Ther.* **12,** 65–77
42. Srinivasan, M., Wardrop, R. M., Gienapp, I. E., Stuckman, S. S., Whitacre, C. C., and Kaumaya, P. T. (2001) *J. Immunol.* **167,** 578–585
43. Srinivasan, M., Gienapp, I. E., Stuckman, S. S., Rogers, C. J., Jewell, S. D., Kaumaya, P. T., and Whitacre, C. C. (2002) *J. Immunol.* **169,** 2180–2188
44. Allen, S. D., Rawale, S. V., Whitacre, C. C., and Kaumaya, P. T. (2005) *J. Pept. Res.* **65,** 591–604
45. Goodman, M., Ro, S., Yamazaki, T., Spencer, J. R., Toy, A., Huang, Z., He, Y., and Reisine, T. (1992) *Bioorg. Khim.* **18,** 1375–1393
46. Sundaram, R., Lynch, M. P., Rawale, S. V., Sun, Y., Kazanji, M., and Kaumaya, P. T. (2004) *J. Biol. Chem.* **279,** 24141–24151
47. Söll, R., and Beck-Sickinger, A. G. (2000) *J. Pept. Sci.* **6,** 387–397
48. Rovero, S., Amici, A., Di Carlo, E., Bei, R., Nanni, P., Quaglino, E., Porcedda, P., Boggio, K., Smorlesi, A., Lollini, P. L., Landuzzi, L., Colombo, M. P., Giovarelli, M., Musiani, P., and Forni, G. (2000) *J. Immunol.* **165,** 5133–5142
49. Chorev, M., and Goodman, M. (1995) *Trends Biotechnol.* **13,** 438–445
50. Chorev, M. (2005) *Biopolymers* **80,** 67–84
51. Wada, T., Qian, X. L., and Greene, M. I. (1990) *Cell* **61,** 1339–1347
52. Franklin, M. C., Carey, K. D., Vajdos, F. F., Leahy, D. J., de Vos, A. M., and Sliwkowski, M. X. (2004) *Cancer Cell* **5,** 317–328
53. Allen, S. D., Garrett, J. T., Rawale, S. V., Jones, A. L., Phillips, G., Forni, G., Morris, J. C., Oshima, R. G., and Kaumaya, P. T. (2007) *J. Immunol.* **179,** 472–482
54. Agus, D. B., Akita, R. W., Fox, W. D., Lewis, G. D., Higgins, B., Pisacane, P. I., Lofgren, J. A., Tindell, C., Evans, D. P., Maiese, K., Scher, H. I., and Sliwkowski, M. X. (2002) *Cancer Cell* **2,** 127–137
55. Nagy, P., Friedländer, E., Tanner, M., Kapanen, A. I., Carraway, K. L., Isola, J., and Jovin, T. M. (2005) *Cancer Res.* **65,** 473–482
56. Baselga, J., and Arteaga, C. L. (2005) *J. Clin. Oncol.* **23,** 2445–2459
57. Baselga, J. (2006) *Science* **312,** 1175–1178
58. Kaumaya, P. T., Foy, K. C., Garrett, J., Rawale, S. V., Vicari, D., Thurmond, J. M., Lamb, T., Mani, A., Kane, Y., Balint, C. R., Chalupa, D., Otterson, G. A., Shapiro, C. L., Fowler, J. M., Grever, M. R., Bekaii-Saab, T. S., and Carson, W. E., 3rd (2009) *J. Clin. Oncol.* **27,** 5270–5277
59. Garrett, J. T., Rawale, S., Allen, S. D., Phillips, G., Forni, G., Morris, J. C., and Kaumaya, P. T. (2007) *J. Immunol.* **178,** 7120–7131
60. Hynes, N. E., and Lane, H. A. (2005) *Nat. Rev. Cancer* **5,** 341–354
61. Hudziak, R. M., Lewis, G. D., Winget, M., Fendly, B. M., Shepard, H. M., and Ullrich, A. (1989) *Mol. Cell. Biol.* **9,** 1165–1172
62. Shepard, H. M., Lewis, G. D., Sarup, J. C., Fendly, B. M., Maneval, D., Mordenti, J., Figari, I., Kotts, C. E., Palladino, M. A., Jr., Ullrich, A., *et al.* (1991) *J. Clin. Immunol.* **11,** 117–127
63. Ryan, A. J., and Wedge, S. R. (2005) *Br. J. Cancer* **92,** S6–S13
64. Li, B., Ogasawara, A. K., Yang, R., Wei, W., He, G. W., Zioncheck, T. F., Bunting, S., de Vos, A. M., and Jin, H. (2002) *Hypertension* **39,** 1095–1100
65. Eskens, F. A., and Verweij, J. (2006) *Eur. J. Cancer* **42,** 3127–3139
66. Grothey, A. (2006) *Oncology* **20,** 21–28
67. Carter, P., Presta, L., Gorman, C. M., Ridgway, J. B., Henner, D., Wong, W. L., Rowland, A. M., Kotts, C., Carver, M. E., and Shepard, H. M. (1992) *Proc. Natl. Acad. Sci. U.S.A.* **89,** 4285–4289
68. Taylor, E. M., Otero, D. A., Banks, W. A., and O'Brien, J. S. (2000) *J. Pharmacol. Exp. Ther.* **295,** 190–194
69. Fischer, P. M. (2003) *Curr. Protein Pept. Sci.* **4,** 339–356
70. Fletcher, M. D., and Campbell, M. M. (1998) *Chem. Rev.* **98,** 763–796
71. Oshima, R. G., Lesperance, J., Munoz, V., Hebbard, L., Ranscht, B., Sharan, N., Muller, W. J., Hauser, C. A., and Cardiff, R. D. (2004) *Cancer Res.* **64,** 169–179
72. Stern, D. F., and Kamps, M. P. (1988) *EMBO J.* **7,** 995–1001
73. Vicari, D., Foy, K. C., Liotta, E. M., and Kaumaya, P. T. P. (2011) *J. Biol. Chem.* **286,** 13612–13625